JAERI-M
9028

A DEVELOPMENT OF NONEQUILIBRIUM ECC MIXING MODEL FOR USE IN ALARM-P1

— DESCRIPTION OF NONEQUILIBRIUM ENERGY EQUATIONS AND IMPLEMENTATION SCHEME TO THE 1V1T CODE, ALARM-P1 —

August 1980

Masayuki AKIMOTO and Fumimasa ARAYA

日本原子力研究所
Japan Atomic Energy Research Institute

JAERI-M 9028

A Development of Nonequilibrium ECC Mixing Model for Use in ALARM-P1

- Description of nonequilibrium energy equations and implementation scheme to the 1V1T code, ALARM-P1 -

Masayuki AKIMOTO and Fumimasa ARAYA

Division of Reactor Safety Evaluation,
Tokai Research Establishment, JAERI

(Received August 8, 1980)

The report presents a model to simulate the nonequilibrium phenomena associated with the mixing of subcooled water with saturated or superheated steam and an implementation scheme of this model to the 1V1T (one velocity and one temperature) code, ALARM-P1. The model, which is able to cover a wide range of thermodynamic nonequilibrium including the meta-stable condition, is based on the 1V2T (one velocity and two temperatures) concept. The energy and mass transfer due to condensation are calculated for each control volume through use of a flow regime dependent constitutive relations. For vertical two phase flow, the existing flow regime map and heat transfer correlations are used to calculate the energy transfer between phases. For horizontal two phase flow, a simple model based on the results of some experiments of direct contact condensation for jet flow is proposed.

Keywords: ECC Mixing, Nonequilibrium, LOCA, PWR, ALARM-P1 Code, Implementation Scheme.

JAERI－M 9028

ＡＬＡＲＭ－Ｐ１のための非平衡ＥＣＣ混合モデルの開発

日本原子力研究所東海研究所安全解析部
秋元　正幸・新谷　文将

（１９８０年８月８日受理）

サブクール水が飽和又は過熱蒸気と混合する場合の熱的非平衡を模擬するモデルを提案し，平衡モデルを採用しているＡＬＡＲＭ－Ｐ１コードへの導入法を示す。このモデルは，擬安定状態を含む熱的非平衡の広い範囲を模擬するものである。二相流の挙動は，一速度二温度（１Ｖ２Ｔ）の基に考えられる。凝縮による相間のエネルギー，質量の輸送は，各コントロールボリウム内で，流れ様式に依存した形で計算される。垂直二相流については，これまで開発された流れ様式図と熱伝達係数コリレイションを用いて，相間の熱移動量が計算される。水平二相流については，関連する実験結果を基に簡単なモデルが提案される。

CONTENTS

LIST OF TABLE

LIST OF FIGURES

目　　次

1. Introduction

In water reactor safety, one of most important nonequilibrium aspects is direct contact condensation, which includes condensation of vapor bubbles or jets in a subcooled liquid pool, condensation of continuous vapor phase on subcooled liquid droplets and condensation at vapor-liquid interface of arbitrary configuration. The rapid condensation may occur near the ECC injection point in the cold leg and the downcomer annulus after the ECC injection starts during a postulated LOCA of a pressurized water reactor (PWR).

In the present version of ALARM-P1[1], the assumption of thermodynamic equilibrium is often unrealistic for the refill phase. As a result of the injection of subcooled water, instantaneous mixing of the subcooled ECC water and resident steam will occure, and the system will be unrealistically depressurized. For such cases, the simple explicit numerical method in ALARM-P1 often fails to proceed due to the numerical instability. Consequently, the calculated liquid temperatures in some parts of the system may greatly differ from actually observed temperatures. For example, a recent LOFT test (L2-2)[2] indicated that water delivered to the lower plenum can be substantially subcooled. This test also showed a cold leg oscillation which began just after ECC injection and lasted for about 30 seconds. This oscillation is understood due to condensation-driven fluid motion. ALARM-P1 or other codes with a complete equilibrium models can not reproduce such observations.

Nonequilibrium condensation models have been incorporated into recently developed advanced system LOCA codes such as TRAC-P1A[3], RELAP5[4] and COBRA-TF[5]. In TRAC-P1A, the condensation rate is calculated by interfacial surface areas and heat transfer coefficients based on flow regime considerations. The TRAC model for condensation assumes that the resistance to the heat transfer is only in the liquid side (the vapor side heat transfer coefficient is always assumed to be a large value of 1×10^4 ($W/m^2/K$)) and the total liquid heat transfer coefficients are those for boiling with appropriate modification. The flow regime may used is based on only vertical two phase flow. In RELAP5, no special constitutive relations for condensation but for vapor generation are incorporated. The model for vapor generation is assumed to be applied to the condensation processes. COBRA-TF using subchannel model is being developed for a hot bundle/hot channel analysis and a water reactor primary system simulation

which is readily able to model complex vessel internal geometries such as those encountered in UHI-equipped PWR's. The condensation model incorporated is focused on the reflood processes in the core region. The validity of this model is not yet extensively tested. RELAP4/MOD7 incorporates a simple nonequilibrium model which is through the use of an equivalent equilibrium system which yields the same depressurization rate as the nonequilibrium system assuming existence of saturated steam. The interfacial heat transfer between phases is determined based on the simplified vertical two phase flow regime map. Other nonequilibrium models have been discussed and proposed by Asahi[7] et al., Jones and Saha[8], and Hughes et al..[9] These models are, for the most part, require specification of empirical relaxation or other constants which must be determined through comparisons of code calculations with experimental data. A model proposed by Hughes[9] is to attempt the calculation of condensation rate by computing meaningful interfacial surface areas and heat transfer coefficients based on both vertical and horizontal flow regimes. Clearly, it cannot be expected that such models are universally applicable to all of the ECC mixing situations likely to occur during PWR LOCA transient. For example, a trigger of instability due to the condensation-driven fluid motion, which occurs in mixing tee,[20),21] is not considered in the system LOCA codes developed so far.

A model, which could cover a wide range of thermodynamic nonequilibrium including the meta-stable, has been formulated based on 1V2T (one velocity-two temperatures) concept. The proposed model allows the coexistence of two phase of unequal temperatures. This coexistence means that the mass and energy transfer between phases are determined by an additional constitutive equation. The model can reproduce the physical situations such as that occuring during ECC injection where subcooled water partialy mixes with saturated or superheated steam. This mixing of subcooled water with steam occurs not only in the cold leg (horizontal flow region) but also in the downcomer (vertical flow region). Nonequilibrium phenomena occuring in such situations are assumed to approach an equilibrium through interfacial mass and energy transfer between phases depending on both vertical and horizontal flow regimes.

In the following section, first the equilibrium model in the present version of ALARM-P1 is reviewed, then nonequilibrium model and its implementation scheme are discussed. In the section 5, correlations for interfacial areas and heat transfer used to determine the condensation rate are presented and a model to simulate instable flow oscillation which

occurs in the ECC mixing tee due to the condensation-driven fluid motion is proposed.

2. ALARM-P1 Equilibrium Model

To describe the thermohydraulic behavior of a PWR reactor system, the system is divided into a number of spatial volume elements called control volume and the conservation equations of mass and energy are solved for each fluid control volume together with one-dimensional momentum balances across the interfaces (junction) between control volumes. The resulting set of simultaneous equations that is based on the assumptions of homogeneous (equal velocities between phases) and thermal-equilibrium (equal temperature between phases) is linearized and integrated for a small time increment by a simple explicit numerical technique.

Neglecting potential and kinetic energy terms and assuming no air present, the conservation equation for mass and energy for control volume i can be written as

$$\frac{d}{dt} M(i) = \sum_j (W_g(j) + W_\ell(j)) , \tag{1}$$

$$\frac{d}{dt} U(i) = \sum_j (W_g(j)h_g(j) + W_\ell(j)h_\ell(j)) . \tag{2}$$

The specific volume at new time level, n+1, $v^{n+1}(i) = V^{n+1}(i)/M^{n+1}(i)$, and the specific internal energy at new time level, n+1, $u^{n+1}(i) = U^{n+1}(i)/M^{n+1}(i)$ can be obtained once equations (1) and (2) are integrated over a time step width $\Delta t(=t^{n+1}-t^n)$. As a result of thermal equilibrium assumptions, all thermodynamic quantities are completely determined by $v^{n+1}(i)$ and $u^{n+1}(i)$. The thermodynamic equilibrium pressure is determined by the following method.

A nonlinear Newton-Raphson iteration method is used to obtain the thermodynamic equilibrium quantities using existing steam table.[22] First of all, we obtain saturated liquid and vapor specific volumes, $v_{\ell s}$ and v_{gs}, corresponding to the internal specific energy, $u^{n+1}(i)$. The iterative solution is based on the function,

$$f(T_s) = u^{n+1}(i) - u_{\ell s}(T_s) , \tag{3}$$

where $u_{\ell s}$ is a saturated liquid specific internal energy and T_s is saturated

occurs in the ECC mixing tee due to the condensation-driven fluid motion is proposed.

2. ALARM-P1 Equilibrium Model

To describe the thermohydraulic behavior of a PWR reactor system, the system is divided into a number of spatial volume elements called control volume and the conservation equations of mass and energy are solved for each fluid control volume together with one-dimensional momentum balances across the interfaces (junction) between control volumes. The resulting set of simultaneous equations that is based on the assumptions of homogeneous (equal velocities between phases) and thermal-equilibrium (equal temperature between phases) is linearized and integrated for a small time increment by a simple explicit numerical technique.

Neglecting potential and kinetic energy terms and assuming no air present, the conservation equation for mass and energy for control volume i can be written as

$$\frac{d}{dt} M(i) = \sum_j (W_g(j) + W_\ell(j)) , \tag{1}$$

$$\frac{d}{dt} U(i) = \sum_j (W_g(j)h_g(j) + W_\ell(j)h_\ell(j)) . \tag{2}$$

The specific volume at new time level, n+1, $v^{n+1}(i) = V^{n+1}(i)/M^{n+1}(i)$, and the specific internal energy at new time level, n+1, $u^{n+1}(i) = U^{n+1}(i)/M^{n+1}(i)$ can be obtained once equations (1) and (2) are integrated over a time step width $\Delta t(=t^{n+1}-t^n)$. As a result of thermal equilibrium assumptions, all thermodynamic quantities are completely determined by $v^{n+1}(i)$ and $u^{n+1}(i)$. The thermodynamic equilibrium pressure is determined by the following method.

A nonlinear Newton-Raphson iteration method is used to obtain the thermodynamic equilibrium quantities using existing steam table.[22] First of all, we obtain saturated liquid and vapor specific volumes, $v_{\ell s}$ and v_{gs}, corresponding to the internal specific energy, $u^{n+1}(i)$. The iterative solution is based on the function,

$$f(T_s) = u^{n+1}(i) - u_{\ell s}(T_s) , \tag{3}$$

where $u_{\ell s}$ is a saturated liquid specific internal energy and T_s is saturated

temperature. A T_s satisfying $f(T_s)=0$ can be obtained using the Newton-Raphson iteration given by,

$$T_s^{r+1} = T_s^r - \frac{f(T_s^r)}{\left.\frac{du_{\ell s}}{dT_s}\right|_{T_s=T_s^r}} \quad . \tag{4}$$

The drivatives is obtained using Clausius-Clapeyron's relation,

$$\frac{du}{dT} = \left(\frac{\partial u}{\partial T}\right)_P + \left(\frac{\partial u}{\partial P}\right)_T \frac{dP}{dT}$$

$$= \left(\frac{\partial h}{\partial T}\right)_P - P\left(\frac{\partial v}{\partial T}\right)_P + \left\{\left(\frac{\partial h}{\partial P}\right)_T - P\left(\frac{\partial v}{\partial P}\right)_T - v\right\} \frac{h_{gs}-h_{\ell s}}{T(v_{gs}-v_{\ell s})}$$

$$= (c_p - Pv\beta) + (Pv\kappa - Tv\beta) \frac{h_{gs}-h_{\ell s}}{T(v_{gs}-v_{\ell s})} \quad . \tag{5}$$

We can also find the saturated liquid specific volume, $v_{\ell s}$, once T_s is obtained. The same procedure as used to obtain $v_{\ell s}$ is adopted to obtain v_{gs}. The thermodynamic condition at new time level, n+1, is determined by comparison of $v^{n+1}(i)$ with $v_{\ell s}$ and v_{gs}. If $v^{n+1}(i)$ is less than $v_{\ell s}$ or greater than v_{gs}, the fluid condition at new time level is single-phase. The fluid is subcooled if $v^{n+1}(i) < v_{\ell s}$ and superheated $v^{n+1}(i) > v_{gs}$. In single-phase volumes, we also use the nonlinear Newton-Raphson iteration to obtain the thermodynamic equilibrium pressure. The iterative solution is based on the functions,

$$f(P,T) = v^{n+1}(i) - v(P,T) \quad ,$$

$$g(P,T) = u^{n+1}(i) - u(P,T) \quad .$$

Using Taylor series expansion around P_i and T_i, above two equations are:

$$f(P,T) = f(P_i,T_i) + \left(\frac{\partial f}{\partial P}\right)_T (P-P_i) + \left(\frac{\partial f}{\partial T}\right)_P (T-T_i) + \ldots \quad , \tag{6}$$

$$g(P,T) = g(P_i,T_i) + \left(\frac{\partial g}{\partial P}\right)_T (P-P_i) + \left(\frac{\partial g}{\partial T}\right)_P (T-T_i) + \ldots \quad , \tag{7}$$

and we set,

$$f_P = \left(\frac{\partial f}{\partial P}\right)_T = -\left(\frac{\partial v}{\partial P}\right)_T + v\kappa \quad , \tag{8}$$

$$f_T = \left(\frac{\partial f}{\partial T}\right)_P = - \left(\frac{\partial v}{\partial T}\right)_P = - v\beta \ , \tag{9}$$

$$g_P = \left(\frac{\partial g}{\partial P}\right)_T = - \left(\frac{\partial u}{\partial P}\right)_T = - \left(\frac{\partial h}{\partial P}\right)_T + P\left(\frac{\partial v}{\partial P}\right)_T + v$$

$$= - v + T\left(\frac{\partial v}{\partial T}\right)_P + P\left(\frac{\partial v}{\partial P}\right)_T + v$$

$$= Tv\beta - Pv\kappa \ , \tag{10}$$

$$g_T = \left(\frac{\partial g}{\partial T}\right)_P = - \left(\frac{\partial u}{\partial T}\right)_P = - \left(\frac{\partial h}{\partial T}\right)_P + P\left(\frac{\partial v}{\partial T}\right)_P$$

$$= - c_p + Pv\beta \ . \tag{11}$$

Eliminating T_i from equations (6) and (7), the Newton-Raphson iteration scheme is obtained:

$$P_{i+1} = P_i - \left[\frac{fg_T - gf_T}{g_T f_P - f_T g_P} \right]_i \ . \tag{12}$$

Eliminating P_i, similar iteration equation for T_i is obtained

$$T_{i+1} = T_i - \left[\frac{gf_P - fg_P}{f_T g_P - g_T f_P} \right]_i \ . \tag{13}$$

If the specific internal volume $v^{n+1}(i)$ is between $v_{\ell s}$ and v_{gs}, the thermodynamic condition is two-phase mixture. Pressure equilibrium is assumed between phases and liquid and vapor are always assumed to be saturated conditions. The iterative solution for equilibrium two phase mixture is based on the functions,

$$f(P,x) = v^{n+1}(i) - [xv_{sg}(P) + (1-x)v_{s\ell}(P)] \tag{14}$$

$$g(P,x) = u^{n+1}(i) - [xh_{sg}(P) + (1-x)h_{s\ell}(P) - Pv^{n+1}(i)] \ , \tag{15}$$

where

x = quality in the volume i,
v_{sg} = saturated steam specific volume,
$v_{s\ell}$ = saturated liquid specific volume,
h_{sg} = saturated steam enthalpy,
$h_{s\ell}$ = saturated liquid enthalpy.

To obtain P and x, similar procedures such as equations (12) and (13) are used with the partial derivatives:

$$f_P = \left(\frac{\partial f}{\partial P}\right)_x = - v_{sg} + v_{s\ell} \quad , \tag{16}$$

$$f_x = \left(\frac{\partial f}{\partial x}\right)_P = - x \frac{dv_{sg}}{dP} - (1-x) \frac{dv_{s\ell}}{dP} \quad , \tag{17}$$

$$g_P = \left(\frac{\partial g}{\partial x}\right)_x = -x \frac{dh_{sg}}{dP} - (1-x) \frac{dh_{s\ell}}{dP} + v^{n+1}(i) \quad , \tag{18}$$

$$g_x = \left(\frac{\partial g}{\partial x}\right)_P = - h_{sg} + h_{s\ell} \quad , \tag{19}$$

and derivatives,

$$\frac{dv}{dP} = \left(\frac{\partial v}{\partial P}\right)_T + \left(\frac{\partial v}{\partial T}\right)_P \frac{dT}{dP}$$

$$= - v\kappa + v\beta T \frac{v_{sg} - v_{s\ell}}{h_{sg} - h_{s\ell}} \quad , \tag{20}$$

$$\frac{dh}{dP} = c_p \frac{dT}{dP} + \left[v - T\left(\frac{\partial v}{\partial T}\right)_P \right]$$

$$= c_p T \frac{v_{sg} - v_{s\ell}}{h_{sg} - h_{s\ell}} + (v - vT\beta) \quad . \tag{21}$$

Under the equilibrium assumptions, the condensation rate can explicitly be obtained using separate mass conservation equations for each phase;

$$\frac{d}{dt} M_g(i) = \sum_j W_g(j) - \dot{M}_{COND}(i) \tag{22}$$

$$\frac{d}{dt} M(i) = \sum_j W_\ell(j) + \dot{M}_{COND}(i) \tag{23}$$

where $\dot{M}_{COND}(i)$ is condensation rate in volume, i. The energy conservation equation for two phase mixture in terms of enthalpy can be expressed:

$$\frac{d}{dt} [M_\ell(i)h_\ell(i)+M_g(i)h_g(i)] - V(i) \frac{dP}{dt} = \sum_j W(j)h(j) + Q(i) \tag{24}$$

where V(i) is volume. From two equations the condensation rate $\dot{M}_{COND}(i)$ is given by,

$$\dot{M}_{COND}(i) = \frac{1}{h_{sg}-h_{s\ell}} \left[\sum_j W_g(j)\{h_{sg}-h_g(j)\} + \sum_j W_\ell(j)\{h_{s\ell}-h_\ell(j)\} \right.$$

$$\left. - Q_i + \{M_g(i) \frac{dh_{sg}}{dP} + M_\ell(i)\frac{dh_{s\ell}}{dP} - V(i)\} \frac{dP(i)}{dt} \right] . \qquad (25)$$

when subcooled water is injected into a volume containing a two phase mixture, the injected liquid instantaneously reaches the saturation state if there is sufficient amount of vapor. This process results in unrealistically high depressurization rates.

3. Nonequilibrium Condensation Model

The nonequilibrium condensation model to be incorporated into ALARM-P1 is based on separate energy conservation equations for each phase. The primary purpose of this model is to eliminate unrealistically rapid depressurization when the ECC water is injected into a primary loop. The model allows the coexistence of steam and water with unequal temperatures in a control volume. This coexistence means that the mass and energy transfer rates between phases is no longer determined only by overall mass and energy conservation principles. An additional constitutive equation is needed to calculate the condensation rate depending on the extent of the departure from equilibrium.

The basic assumption invoked in the nonequilibrium model are as follows:

(1) Steam and water with unequal temperatures can coexist within a control volume although each phase is homogeneous. That means incoming liquid completely mixes with the resident liquid and incoming vapor completely mixes with the resident vapor.

(2) For two phase mixture, pressure equilibrium is assumed between phases. The allowable thermodynamic states of interest include:

(i) liquid phase only,
  subcooled liquid,
  saturated liquid,
  superheated liquid,

(ii) vapor phase only,
  subcooled steam,
  saturated steam,
  superheated steam,

$$\dot{M}_{COND}(i) = \frac{1}{h_{sg}-h_{s\ell}} \left[\sum_j W_g(j)\{h_{sg}-h_g(j)\} + \sum_j W_\ell(j)\{h_{s\ell}-h_\ell(j)\} \right.$$

$$\left. - Q_i + \{M_g(i) \frac{dh_{sg}}{dP} + M_\ell(i)\frac{dh_{s\ell}}{dP} - V(i)\} \frac{dP(i)}{dt} \right] . \qquad (25)$$

when subcooled water is injected into a volume containing a two phase mixture, the injected liquid instantaneously reaches the saturation state if there is sufficient amount of vapor. This process results in unrealistically high depressurization rates.

3. Nonequilibrium Condensation Model

The nonequilibrium condensation model to be incorporated into ALARM-P1 is based on separate energy conservation equations for each phase. The primary purpose of this model is to eliminate unrealistically rapid depressurization when the ECC water is injected into a primary loop. The model allows the coexistence of steam and water with unequal temperatures in a control volume. This coexistence means that the mass and energy transfer rates between phases is no longer determined only by overall mass and energy conservation principles. An additional constitutive equation is needed to calculate the condensation rate depending on the extent of the departure from equilibrium.

The basic assumption invoked in the nonequilibrium model are as follows:

(1) Steam and water with unequal temperatures can coexist within a control volume although each phase is homogeneous. That means incoming liquid completely mixes with the resident liquid and incoming vapor completely mixes with the resident vapor.

(2) For two phase mixture, pressure equilibrium is assumed between phases. The allowable thermodynamic states of interest include:

(i) liquid phase only,
subcooled liquid,
saturated liquid,
superheated liquid,

(ii) vapor phase only,
subcooled steam,
saturated steam,
superheated steam,

and various mixtures of two states from each phase.

(3) The thermodynamic quantities for subcooled vapor and superheated liquid are assumed to be extrapolated values from the saturate values.

(4) The condensation rate is governed by the degree of temperature difference between phases, interfacial area within a volume, A_i and liquid-vapor side interfacial heat transfer coefficients $h_{i\ell}$, h_{iv}. The interfacial mass transfer rate, $\dot{M}_{COND}$ is obtained from a simple energy balance at the interface:

$$\dot{M}_{COND} = \frac{q_{iv} + q_{i\ell}}{h_{fg}} \tag{26}$$

and the interfacial heat transfer, q_{iv} and $q_{i\ell}$ are given by:

$$q_{iv} = h_{iv} A_i (T_s - T_v) , \tag{27}$$

and

$$q_{i\ell} = h_{i\ell} A_i (T_s - T_\ell) . \tag{28}$$

where T_v and T_ℓ are vapor and liquid phase temperature, respectively.

Another model to calculate the condensation rates will be provided. This model is a relaxation model for nonequilibrium condensation flow:

$$\frac{d}{dt} \dot{M}_{COND} = \frac{\dot{M}_{COND,e} - \dot{M}_{COND}}{\tau} \tag{29}$$

where $\dot{M}_{COND,e}$ is an equilibrium condensation rate given by Eq. (25) and τ is a time constant. Condensation is assumed to start at time zero at a rate smaller than $\dot{M}_{COND,e}$, and finally relaxed to the equilibrium state, controlled by the time constant τ.

For this simplified nonequilibrium model, thermodynamic quantities of each phase can be calculated based on the separate mass and energy balances of liquid and vapor, the constant volume assumption and the equations of state. The mass balance equations are the same as equations (22) and (23):

$$\frac{dM_g(i)}{dt} = \sum_j W_g(j) - \dot{M}_{COND}(i) , \tag{22}$$

$$\frac{dM_\ell(i)}{dt} = \sum_j W_\ell(j) + \dot{M}_{COND}(i) . \tag{23}$$

The energy balance equations with neglecting wall heat transfer are

$$\frac{dU_g(i)}{dt} = \sum_j W_g(j)\, h_g(j) + q_{iv} - \dot{M}_{COND}(i)\, h_{sg} \quad , \tag{30}$$

$$\frac{dU_\ell(i)}{dt} = \sum_j W_\ell(j)\, h_\ell(j) + q_{i\ell} + \dot{M}_{COND}(i)\, h_{s\ell} \quad . \tag{31}$$

The mass and internal energy in a volume at a new time level, n+1 are obtained once mass and energy equations are integrated over one time step. All thermodynamic quantities at new time level can be obtained from $M_g^{n+1}(i)$, $M_\ell^{n+1}(i)$, $U_g^{n+1}(i)$ and $U_\ell^{n+1}(i)$.

4. Implementation Scheme

An implementation of the nonequilibrium model which is able to cover wide range of thermal nonequilibrium requires a solution scheme completely different from that for equilibrium condition. A solution procedure to obtain all other thermodynamic quantities than M_g^{n+1}, M_ℓ^{n+1}, U_g^{n+1} and U_ℓ^{n+1} using existing steam table is described below.

A nonlinear Newton-Raphson iteration loop is used to obtain the pressure. For this iteration, the old time value is used as a first iterate value, and iteration continues until the required input convergence criterion is met, or iteration limit is exceeded.

First, saturation quantities of vapor and liquid phase corresponding to $U_g^{n+1}(i)/M_g^{n+1}(i)$ and $U_\ell^{n+1}(i)/M_\ell^{n+1}(i)$, respectively, are obtained using the Newton-Raphson iteration loop. The iterative solution is based on the function,

$$f(T_s) = u_g^{n+1}(i) - u_{gs}(T_s) \quad , \tag{32}$$

where T_s is a saturation temperature corresponding to the vapor specific internal energy u_g^{n+1}. The iteration scheme is given by

$$T_s^{r+1} = T_s^r - \frac{f(T_s^r)}{\left(\frac{du_{gs}}{dT_s}^r\right)} \tag{33}$$

and

$$\frac{dU_g(i)}{dt} = \sum_j W_g(j)\, h_g(j) + q_{iv} - \dot{M}_{COND}(i)\, h_{sg} \quad , \tag{30}$$

$$\frac{dU_\ell(i)}{dt} = \sum_j W_\ell(j)\, h_\ell(j) + q_{i\ell} + \dot{M}_{COND}(i)\, h_{s\ell} \quad . \tag{31}$$

The mass and internal energy in a volume at a new time level, n+1 are obtained once mass and energy equations are integrated over one time step. All thermodynamic quantities at new time level can be obtained from $M_g^{n+1}(i)$, $M_\ell^{n+1}(i)$, $U_g^{n+1}(i)$ and $U_\ell^{n+1}(i)$.

4. Implementation Scheme

An implementation of the nonequilibrium model which is able to cover wide range of thermal nonequilibrium requires a solution scheme completely different from that for equilibrium condition. A solution procedure to obtain all other thermodynamic quantities than M_g^{n+1}, M_ℓ^{n+1}, U_g^{n+1} and U_ℓ^{n+1} using existing steam table is described below.

A nonlinear Newton-Raphson iteration loop is used to obtain the pressure. For this iteration, the old time value is used as a first iterate value, and iteration continues until the required input convergence criterion is met, or iteration limit is exceeded.

First, saturation quantities of vapor and liquid phase corresponding to $U_g^{n+1}(i)/M_g^{n+1}(i)$ and $U_\ell^{n+1}(i)/M_\ell^{n+1}(i)$, respectively, are obtained using the Newton-Raphson iteration loop. The iterative solution is based on the function,

$$f(T_s) = u_g^{n+1}(i) - u_{gs}(T_s) \quad , \tag{32}$$

where T_s is a saturation temperature corresponding to the vapor specific internal energy u_g^{n+1}. The iteration scheme is given by

$$T_s^{r+1} = T_s^r - \frac{f(T_s^r)}{\left(\frac{du_{gs}}{dT_s}^r\right)} \tag{33}$$

and

$$\frac{du}{dT} = \left(\frac{\partial u}{\partial T}\right)_P + \left(\frac{\partial u}{\partial P}\right)_T \frac{dP}{dT}$$

$$= \left(\frac{\partial h}{\partial T}\right)_P - P\left(\frac{\partial v}{\partial T}\right)_P + \left\{\left(\frac{\partial h}{\partial P}\right)_T - P\left(\frac{\partial v}{\partial P}\right)_T - v\right\} \frac{h_{gs}-h_{\ell s}}{T(v_{gs}-v_{\ell s})}$$

$$= (c_p - Pv\beta) + (Pv\kappa - Tv\kappa) \frac{h_{gs}-h_{\ell s}}{T(v_{gs}-v_{\ell s})} \qquad (34)$$

The same procedure as above scheme is used to obtain saturation temperature corresponding to the specific internal liquid energy u_ℓ^{n+1}. Through these procedures, we can also find all other saturation quantities than temperatures from the steam table.

The iterative solution for the pressure is based on the function with the constant volume assumption,

$$F = v_g(P, u_g^{n+1}) \cdot M_g^{n+1} + v_\ell(P, u_\ell^{n+1}) \cdot M_\ell^{n+1} - V(i) \qquad (35)$$

The Newton-Raphson iteration is given by

$$P^{r+1} = P^r - \frac{F(P^r)}{\left(\frac{\partial F}{\partial P^r}\right)} \quad , \qquad (36)$$

and

$$\left(\frac{\partial F}{\partial P^r}\right) = M_g^{n+1} \left(\frac{\partial v_g}{\partial P^r}\right)_{u_g} + M_\ell^{n+1} \left(\frac{\partial v_\ell}{\partial P^r}\right)_{u_\ell} \quad . \qquad (37)$$

The partial derivatives are

$$\left(\frac{\partial v}{\partial P}\right)_u = -\left(\frac{\partial u}{\partial P}\right)_v \left(\frac{\partial v}{\partial u}\right)_P = -\frac{\left(\frac{\partial u}{\partial T}\right)_v \left(\frac{\partial v}{\partial T}\right)_P}{\left(\frac{\partial P}{\partial T}\right)_v \left(\frac{\partial u}{\partial T}\right)_P} = -\frac{c_v v\kappa}{c_p - v\beta P} \quad . \qquad (38)$$

If the current pressure P^r or converged pressure is greater than the saturation pressure of vapor phase corresponding the internal specific energy u_g^{n+1}, the vapor is assumed to be subcooled state. Temperature and specific volume of subcooled vapor approximated using extrapolation of saturate condition are given by,

$$T_g = T_{gs} + (P^r - P_{gs}) \cdot \left(\frac{\partial T_g}{\partial P_{gs}}\right)_{u_g} \quad , \qquad (39)$$

and

$$v_g = v_{gs} + (P^r - P_{gs}) \cdot \left(\frac{\partial v_g}{\partial P_{gs}} \right)_{u_g} , \tag{40}$$

where T_{gs}, P_{gs} and v_{gs} are saturation temperature, pressure and specific volume of vapor phase, respectively, corresponding to the specific internal energy of vapor, u_g^{n+1}. The partial derivatives are given by

$$\begin{aligned} \left(\frac{\partial T}{\partial P}\right)_u &= - \left(\frac{\partial u}{\partial P} \right)_T \left(\frac{\partial T}{\partial u} \right)_P \\ &= - \left[\left(\frac{\partial h}{\partial P} \right)_T - P \left(\frac{\partial v}{\partial P} \right)_T - v \right] \times \frac{1}{\left(\frac{\partial h}{\partial T} \right)_P - P \left(\frac{\partial v}{\partial T} \right)_P} \\ &= \frac{Tv\beta - Pv\kappa}{c_p - Pv\beta} , \end{aligned} \tag{41}$$

and

$$\begin{aligned} \left(\frac{\partial v}{\partial P} \right)_u &= - \left(\frac{\partial u}{\partial P} \right)_v \left(\frac{\partial v}{\partial u} \right)_P \\ &= \frac{\left(\frac{\partial u}{\partial T} \right)_v \left(\frac{\partial v}{\partial T} \right)_P}{\left(\frac{\partial v}{\partial T} \right)_P \left(\frac{\partial P}{\partial v} \right)_T \left[\left(\frac{\partial h}{\partial T} \right)_P - P \left(\frac{\partial v}{\partial T} \right)_P \right]} \\ &= - \frac{c_v v\beta}{\frac{\beta}{\kappa} (c_p - Pv\beta)} . \end{aligned} \tag{42}$$

Similarly, temperature and specific volume of superheated liquid when the current pressure, P^r or converged pressure is less than the saturation pressure of liquid phase are given by,

$$T_\ell = T_{\ell s} + (P^r - P_{\ell s}) \left(\frac{\partial T_\ell}{\partial P_{\ell s}} \right)_{u_\ell} , \tag{43}$$

$$v_\ell = v_{\ell s} + (P^r - P_{\ell s}) \left(\frac{\partial v_\ell}{\partial P_{\ell s}} \right)_{u_\ell} . \tag{44}$$

where $T_{\ell s}$, $P_{\ell s}$ and $v_{\ell s}$ also are saturation temperature, pressure and specific volume of liquid phase, respectively. The partial derivatives are described with similar formulas to the equations (41) and (42).

5. Constitutive Relations

The conservation equations of mass and energy require certain auxiliary or constitutive equations to effect closure. The models provided to calculate interfacial mass and energy transfer are described below.

The interfacial areas and heat transfer coefficients are determined depending on the change of two-phase flow regime. Many flow regime maps have been proposed. But the logical method to determine flow regime is through various transition criteria from phenomelogical consideration. The criteria obtained so far were basically of adiabatic models. For two-phase flow with phase change, the flow regime is constantly changing and developing due to flow accelaration, nonhomogeneity and nonequilibrium. For such cases, no definite criteria can be formulated. In the advanced codes such as TRAC-P1A, a simplified flow regime map based on the work of Bennett et al.[10] for vertical two phase flow is used. Other advanced codes, RELAP5 and COBRA-TF also use the similar map to that in TRAC-P1A.

For vertical two phase flow, the flow regime map used in the present model also is a simple one, constructed in a similar manner to those in use by other codes. This map is shown in figure 1. This map has the cordinates of homogeneous void fraction α, for the abscissa and total mass flux, G, for the ordinate. The map is assumed to be valid for vertical cocurrent upflow and downflow. Countercurrent annular (liquid on wall) is not considered yet in the present model. For this flow regime, recent experiments in Creare Inc. and Battelle Columbus Laboratories may be useful. As shown in Figure 1 the flow map includes bubbly flow, slug flow, annular flow and droplet flow. In table 1, interfacial flow areas for various flow regimes are shown. The bubbly regime is used up to a void fraction of 0.2 and is assumed to consist of spherical bubbles whose radius is determined from a critical Weber number, We_b,

$$r_b = \frac{1}{2} \frac{We_b \sigma}{\rho_\ell V_r^2} \quad , \tag{45}$$

where r_b is the bubble diameter, σ is surface tension and V_r is relative velocity between phases. For this radius, a uniform bubble distribution within a volume is assumed. The relative velocity is based on Zuber's drift[11] velocity;

$$V_r = \frac{1.41}{(1-\alpha)} \left[\frac{\sigma g(\rho_\ell - \rho_g)}{\rho_\ell^2} \right]^{\frac{1}{2}} . \quad (46)$$

At present a critical Weber number of 8.0[21] is used. The interfacial heat transfer for liquid side is

$$h_{i\ell} = k_\ell \left[\frac{2|V_r| \; 0.25 P_r^{-0.33}}{\pi a_\ell r_b} \right]^{\frac{1}{2}} , \quad (47)$$

and

$$a_\ell = k_\ell / c_{p\ell} \rho_\ell .$$

For the vapor side heat transfer, conduction may be major mechanism. For quasi-steady state, the heat transfer coefficient is[12),13)]

$$h_{iv} = \frac{\pi^2}{3} \frac{k_v}{r_b} . \quad (48)$$

For the annular flow regime, the interphase heat transfer is based on conduction in the liquid film,

$$h_{i\ell} = \frac{k_\ell}{\delta} , \quad (49)$$

where δ is the liquid film thickness given by

$$\delta = \frac{D}{2} (1 - \sqrt{\alpha}) \quad (50)$$

The heat transfer through the vapor core and liquid film is given by the Dittus-Boelter correlation[14)],

$$h_{iv} = \frac{k_v}{2(R-\delta)} \left[0.023 \, R_e^{0.8} P_r^{0.4} \right] . \quad (51)$$

The Reynolds and Prandtl numbers are given by

$$R_e = \frac{\rho_v |V_r| \; 2 \; (R-\delta)}{\mu_v} , \quad (52)$$

$$P_r = \frac{c_{pv} \mu_v}{k_v} . \quad (53)$$

The relative velocity to calculate the Reynolds number is given by M. Ishii's correlation,[15)]

$$V_r = \frac{V_m}{\left[\frac{\rho_g(76-75\alpha)}{\rho_\ell\sqrt{\alpha}}\right]^{\frac{1}{2}} + \frac{\alpha\rho_g}{\rho_m}} \quad . \tag{54}$$

In the droplet flow regime, the heat transfer mechanism occurs between the droplet and a continuous vapor field. The droplet conduction from the surface to the droplet bulk has the coefficient for heat transfer,[13)]

$$h_{i\ell} = \frac{\pi^2}{3}\frac{k_\ell}{r_d} \quad . \tag{55}$$

The convection from the vapor to the droplet, the Frossling equation is used:[16)]

$$h_{iv} = \frac{k_v}{r_d}\left[1 + 0.37\, R_e^{0.5}\, P_r^{\frac{1}{3}}\right] \quad , \tag{56}$$

where

$$R_e = \frac{2\rho_v|V_r|r_d}{\mu_v} \quad , \tag{57}$$

and

$$P_r = \frac{c_{pv}\,\mu_v}{k_v} \quad . \tag{58}$$

The relative velocity to calculate the Reynolds number also is Zuber's drift velocity and the droplet radius is based on the critical Weber number of 12.0[21)].

The slug and annular-mist flow regimes are considered to be transition regions from bubbly to annular and from annular to mist flow regime, respectively. Therefore for the transition region the interpolation procedure is derived using following approach. Supose that control volume V(i) is divided into two parts: for the slug regime, one part contains fluid in bubbly flow with void fraction α_1 and volume V_1 and the remainder of the volume contains fluid in annular flow with void fraction α_2 and volume V_2. Then, the volumes of the bubbly and annular regions can be obtained from the equations;

$$V_1 + V_2 = V(i) \quad , \tag{59}$$

$$\alpha_1 V_1 + \alpha_2 V_2 = \alpha V(i) \quad , \tag{60}$$

where α is the average void fraction of a control volume V(i). The void

fraction α_1 and α_2 are assumed to be the intercepts of the line of constant mass flux with the flow regime boundaries as shown in figure 1. The interfacial areas in divided two subvolumes can be obtained using α_1, α_2, V_1 and V_2 (see table 1). The heat transfer coefficients for two subvolumes also are obtained using the same procedures as described in early part of this section. In the annular-mist region, the similar procedures are used.

For the horizontal flow, the Baker map[17] or the Govier and Aziz map[18] may used. But the coordinates of these two maps basically are dependent on the vapor phase velocity (ordinate) and the liquid phase velocity (abscissa). Each phase velocity in a volume can not be obtained within the limitation of the present 1V2T model. In the present version, a straightforward model is proposed. The nonequilibrium condensation is considered only in the cold leg including ECC injection point. The cold leg of a PWR is a horizontal pipe with steam flow and with subcooled liquid injected into it through a smaller pipe as illustrated in figure 2. Aoki, et al.[19] have studied the condensation of steam injected inside a concurrent subcooled water steam flowing horizontally through a 50 × 20 mm rectangular duct at atomospheric pressure. They found four modes of fluid motion; (i) oscillation of liquid plug between upsteam and downstream of the injection location with low-frequency pressure oscillation; (ii) oscillation of liquid plug in the downstream of the injection location with high-frequency pressure oscillation; (iii) relatively stationary interface in the downstream with irregular pressure fluctuation; (iv) interface excursion including jet, liquid droplet and wavy flow. Their major findings are summarized in figure 4. Block[20] also reported similar findings of Westendrof & Brown's work in jet condensation study and cold leg flow regime map as shown in figure 3 based on experiments by a variety of researchers at a range of scale from 1/20 to 1/30 of PWR scale. There is consistency between Aoki and Block's reports. Block briefly reported an "on-off" model of condensation developed by Rothe et al. This model could predict the complicated lines between the three primary regimes (no liquid plug, hysteresis and oscillatory liquid plug regimes) of behavior shown on figure 3.

Aoki, et al.[19] reported that the transition from the oscillation of liquid plug to the interface excursion can be expressed in terms of the condensation rate at the limit necessary to achieve thermodynamic equilibrium;

$$W_g = 0.84\, M_{c,max} \quad , \tag{61}$$

where W_g is inlet steam mass flow rate and $M_{c,max}$ is given by,

$$M_{c,max} = \frac{W_\ell c_{p\ell}(T_s - T_\ell)}{h_{\ell g}} \quad . \tag{62}$$

Subscripts ℓ, g and s stand for liquid, vapor and saturation, respectively. W_ℓ is injected liquid mass flow rate, c is specific heat, h is latent heat and T is temperature. The quantity of $M_{c,max}/W_g$ is the same one as the thermodynamic ratio R_T proposed by J.A. Block. Aoki, et al. also suggested that the flow is stable (interface excursion) when W_g 0.84 $M_{c,max}$ and the flow is oscillatory (liquid plug oscillation) when $W_g < 0.84\ M_{c,max}$. Under certain conditions the steam is expected to be supherheated, then the equation (64) is extended as

$$M_{c,max} = \frac{W_\ell c_{p\ell}(T_s - T_\ell) + W_g c_{pg}(T_s - T_g)}{h_{\ell g}} \quad . \tag{63}$$

It should be noted that the numerator of this equation is equivalent to the sum of the first and the second term in the right hand side of the equation (25). The $M_{c,max}$ means equilibrium condensation rate with neglecting wall heat transfer and contribution due to depressurization.

The condensation rate and interfacial heat transfer are calculated for the stable flow and the oscillatory flow as follows;

(i) For oscillatory flow, the condensation rate is calculated depending on the liquid fraction in the volume to which the ECC injection pipe is connected. When the interface moves to up stream of the injection location, the cold ECC jet is covered with liquid plug and the interface warms rapidly to the saturation temperature. Condensation ceases and pressure in the volume 1 in figure 2 builds up. Due to this pressure build up, the liquid plug moves to downstream of the injection location, the steam can condense rapidly on the exposed cold jet and this reduces the pressure in the volume 1. These processes cause oscillatory liquid plug. When the liquid fraction, $1-\alpha$, in the volume 1 is greater than the reference liquid fraction, $1-\alpha^*$, which can be calculated from the geometry of the volume 1, the condensation rate in the volume 1 is assumed to be zero;

$$q_{iv} = q_{i\ell} = 0 \ . \tag{64}$$

The equilibrium condensation is assumed when the liquid fraction is smaller than the reference liquid fraction, $1-\alpha^*$;

$$q_{i\ell} = W_\ell c_{p\ell}(T_s - T_\ell) = W_\ell(h_{\ell s} - h_\ell) \ , \tag{65}$$

and

$$q_{iv} = W_g c_{pg}(T_s - T_g) = W_g(h_{gs} - h_g) \ , \tag{66}$$

where W_ℓ is the mass flow rate from the ECC injection pipe and W_g is incoming steam mass flow.

(ii) For the interface excursion, the flow regime includes the two dimensional jet, the liquid droplet due to the atomization of liquid jet and the wavy flow reported by S. Aoki et al. In this straight forward model, the interfacial exchange due to liquid droplet is only assumed in the downstream, volume 2 in figure 2. The calculation procedure is assumed to be the same way as those for the vertical droplet flow. In the volume 2, zero condensation rate is assumed. The assumption will cause large condensation rate than that in the actual situation since the liquid film is neglected and all liquid is assumed to contribute to the atomization. The atomization rate, the droplet size spectra and the coexistence of drop and film flow should be considered.

6. Conclusion

A model proposed within the assumption of 1V2T may be applicable for eliminating unrealistic depressurization as calculated so far during periods of ECC injection. The model including constitutive relations should be checked through appropriate experiments although it contains rough hydrodynamic model due to the limitation of one-velocity model. In particular, for flow regime maps, it will be necessary to make sure that the corresponding interfacial areas and heat transfer correlations are useful in physical processes concerned. The processes of direct contact condensation influence, and are in turn influenced by, fluid motions. Specifically, the friggering of instability in which condensation heat transfer might be a controlling process should appropriately be taken into account for the ECC mixing analysis in mixing tee, downcomer and upper plenum.

Recently Block suggested a universal regime map for direct contact contact condensation. However, that is quite qualitative one and dimensional values as cordinates are used. The use of dimensional coordinates for

$$q_{i\ell} = W_\ell c_{p\ell}(T_s - T_\ell) = W_\ell(h_{\ell s} - h_\ell) \ , \tag{65}$$

and

$$q_{iv} = W_g c_{pg}(T_s - T_g) = W_g(h_{gs} - h_g) \ , \tag{66}$$

where W_ℓ is the mass flow rate from the ECC injection pipe and W_g is incoming steam mass flow.

(ii) For the interface excursion, the flow regime includes the two dimensional jet, the liquid droplet due to the atomization of liquid jet and the wavy flow reported by S. Aoki et al. In this straight forward model, the interfacial exchange due to liquid droplet is only assumed in the downstream, volume 2 in figure 2. The calculation procedure is assumed to be the same way as those for the vertical droplet flow. In the volume 2, zero condensation rate is assumed. The assumption will cause large condensation rate than that in the actual situation since the liquid film is neglected and all liquid is assumed to contribute to the atomization. The atomization rate, the droplet size spectra and the coexistence of drop and film flow should be considered.

6. Conclusion

A model proposed within the assumption of 1V2T may be applicable for eliminating unrealistic depressurization as calculated so far during periods of ECC injection. The model including constitutive relations should be checked through appropriate experiments although it contains rough hydrodynamic model due to the limitation of one-velocity model. In particular, for flow regime maps, it will be necessary to make sure that the corresponding interfacial areas and heat transfer correlations are useful in physical processes concerned. The processes of direct contact condensation influence, and are in turn influenced by, fluid motions. Specifically, the friggering of instability in which condensation heat transfer might be a controlling process should appropriately be taken into account for the ECC mixing analysis in mixing tee, downcomer and upper plenum.

Recently Block suggested a universal regime map for direct contact contact condensation. However, that is quite qualitative one and dimensional values as cordinates are used. The use of dimensional coordinates for

correlation of empirical data raises a scaling problem of the results. In future study, a development of reliable flow regime map which can universally be applicable to two-phase flow transient within an accuracy required by LOCA analysis is one of the most important areas.

ACKNOWLEDGMENT

Appreciation is expressed to K. Sato, the chief of Reactor Safety Code Development Laboratory for his critical reading of this report.

correlation of empirical data raises a scaling problem of the results. In future study, a development of reliable flow regime map which can universally be applicable to two-phase flow transient within an accuracy required by LOCA analysis is one of the most important areas.

ACKNOWLEDGMENT

Appreciation is expressed to K. Sato, the chief of Reactor Safety Code Development Laboratory for his critical reading of this report.

NOMENCLATURE

A_i	Interfacial Area within a volume
c_p	Specific heat at constant pressure
h_{iv}	Interfacial heat transfer for vapor side
$h_{i\ell}$	Interfacial heat transfer for liquid side
h	Specific enthalpy
i	Volume number
j	Junction number
G	Mass velocity
k	Thermal conductivity
M	Total fluid mass in a control volume
M_{COND}	Condensation in a control volume
P	Pressure
Q	Wall heat transfer rate
r_b	Bubble radius
r_d	Droplet radius
T	Temperature
q	Interfacial heat transfer rate
U	Total internal energy in a control volume
V	Total volume of a control volume
v	Specific volume of the fluid
V_r	Relative velocity between phases
W	Mass flow rate
x	quality

Greek Letters

α	Void fraction
β	Coefficient of thermal expansion $\frac{1}{v}(\frac{\partial v}{\partial T})_P$
κ	Isothermal compressibility $-\frac{1}{v}(\frac{\partial v}{\partial P})_T$
σ	Surface tension

Subscripts

g	Vapor phase
ℓ	Liquid phase
s	Saturation state

REFERENCES

1) M. AKIMOTO, et al., "ALARM-P1 : A Computer Program for Pressurized Water Reactor Blowdown Analysis", JAERI-M-8004, Dec. 1978.
2) D.L. Batt, "Quick Look Report on LOFT Nuclear Experiment L2-2." LOFT-TR-103, Dec. 1978.
3) D.R. Liles, et al., "TRAC-P1A, An Advanced Best-Estimate Computer Program for PWR LOCA Analysis, Volume I", LASL Draft, 1979.
4) V.H. Ranson, et al., "RELAP5 Code Description", CDAP-TR-78-035, Aug. 1978.
5) M.J. Thurgood and J.M. Kelly, "COBRA-TF MODEL Description", Prepared for the NRC Advanced Code Review Group Meeting January 24 and 25., Dec. 1979.
6) S.R. Fischer et al., "Development of a Nonequilibrium ECC Mixing Model for use in RELAP4/MOD7", MIAMI, two phase conference handout, Apr. 1979.
7) Y. Asahi, M. Hirano and K. Sato, "Brief Description of the THYDE-P Code", Presented at the JAERI/LOFT Meeting in JAPAN, Mar. 1980.
8) O.C. Jones and P. Saha, "Non-equilibrium Aspects of Water Reactor Safety", BNL-NUREG 23143, July 1977.
9) E.D. Hughes, "Development of Multi-Fluid Models of Two-Phase Flow for Reactor Analysis", EI-79-6, Mar. 1979.
Prepared for JAERI.
10) A.W. Bennett et al., "Flow Visualization Studies of Boiling Water at High Pressure" ADRE-R 4874, 1965.
11) N. Zuber and J.A. Findlay, "Average Volumetri Concentration in Two-Phase Flow System", Journal of Heat Transfer, Nov. 1965 (453-468).
12) D. Moalem and S. Sideman, "The Effect of Motion on Bubble Collapse", Int. J. Heat Mass Transfer, Vol. 16, 2321-2324, 1973.
13) R.B. Bird, et al., "Transport Phenomena", John Wiley & Sons, Inc. 1962.
14) F.W. Dittus and L.M.K. Boelter, "Heat Transfer in Automobile Radiator of Tubular Type", University of California Publications in Engineering, Vol. 2, 1930.
15) M. Ishii, "Light Water-Reactor Safety Research Program: Quarterly Progress Report", Oct.-Dec. 1976, ANL-77-10, Mar. 1977.
16) N.A. Fuchs, "Evaporation and Droplet Growth in Gaseous Media", Pergamo Press, Great Britain, 1959. or P.N. Rowe, et al., "Heat

Transfer from a Single Sphere in a Extensive Flowing Fluid", Trans. Instn. Chem. Engrs., 43, T14-T31, 1965.

17) O. Baker, "Simultaneous Flow of Oil and Gas", Oil and Gas Journal, Vol. 53, 185-189, 1954.

18) G.W. Govier and K. Aziz, "The flow of Complex Mixtures in Pipes", Van Nostrand Reinhold Co. New York, 1972.

19) S. Aoki, et al., "Study on Cooling Effect of Injection of the Emergency Cooling System in Nuclear Reactor" (In Japanese), Prepared for JAERI under contract between TIT and JAERI, Mar. 1980.

20) J.A. Block, "Condensation-Driven Fluid Motions", Int. J. Multiphase Flow, Vol. 6, pp.113-129, 1980.

21) G.B. Wallis, "One-dimensional Two-phase Flow", McGraw-Hill Book Company, 1969.

TABLE 1 Interfacial Heat Transfer Areas for Vertical Two-Phase Flow

Flow Regime	Interfacial Area, A_i
Bubbly	$\frac{3\alpha}{r_b}$ * Vol (i)
Slug	Interpolation of bubbly and annular flow
Annular	$\frac{4\sqrt{\alpha}}{D}$ * Vol(i)
Drop	$\frac{3(1-\alpha)}{r_d}$ * Vol (i)

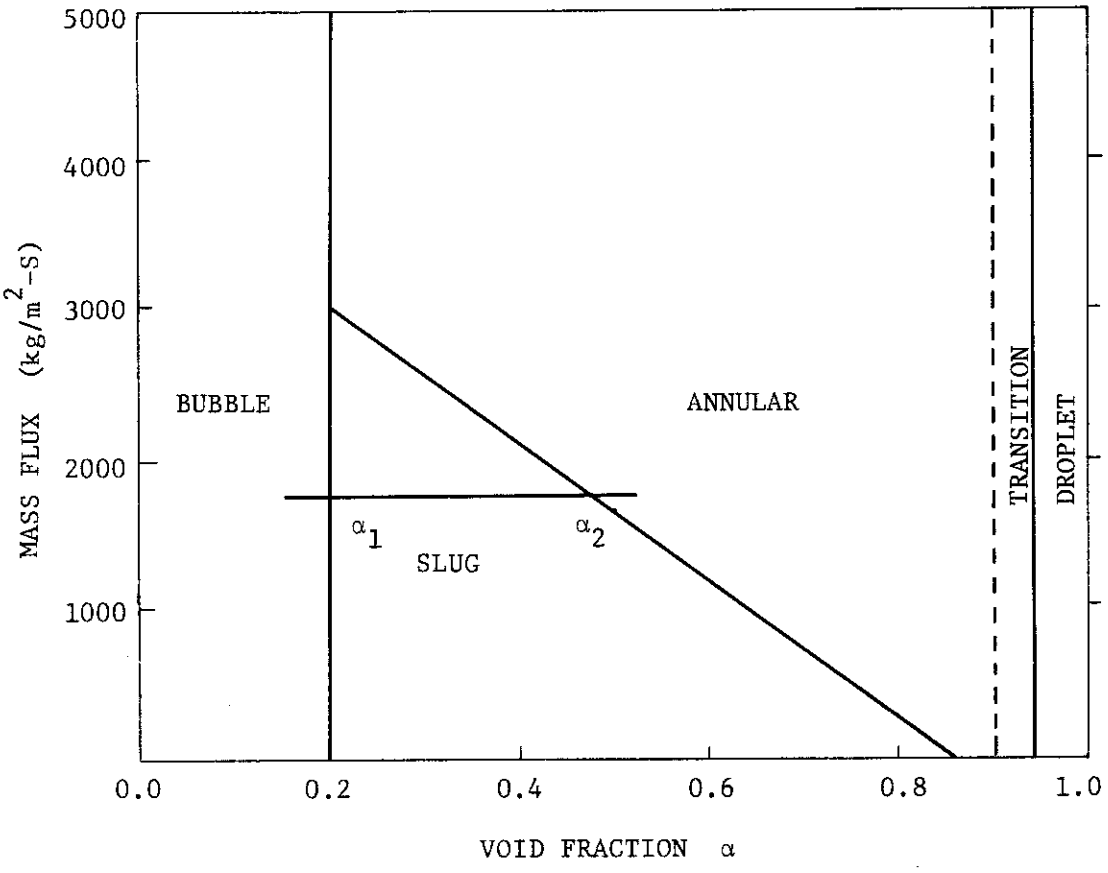

Figure 1 Modified Bennett flow regime map for vertical flow

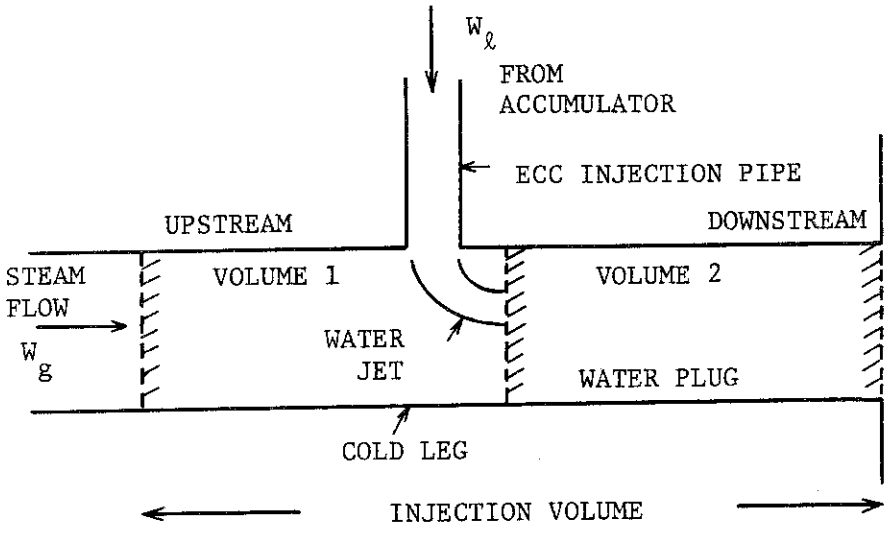

Figure 2 Model for analysis of ECC mixing in cold leg.

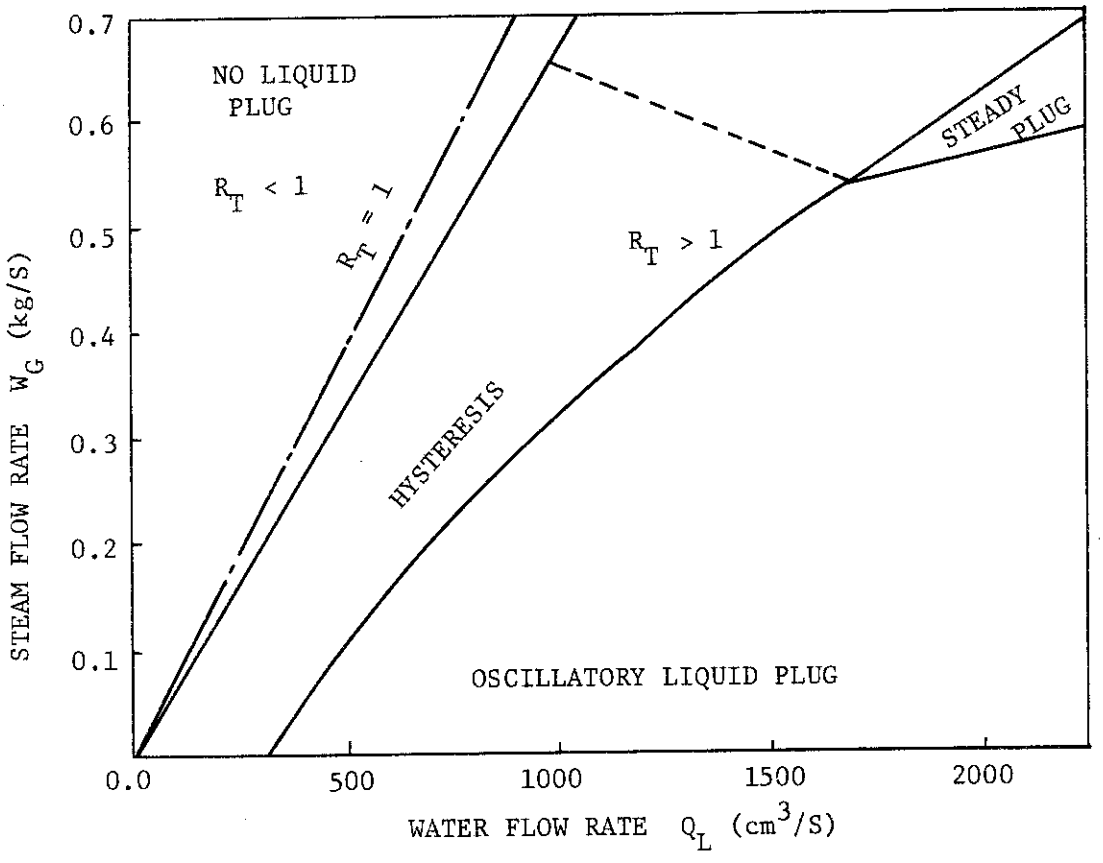

Figure 3 Cold leg flow regime map from reference 20

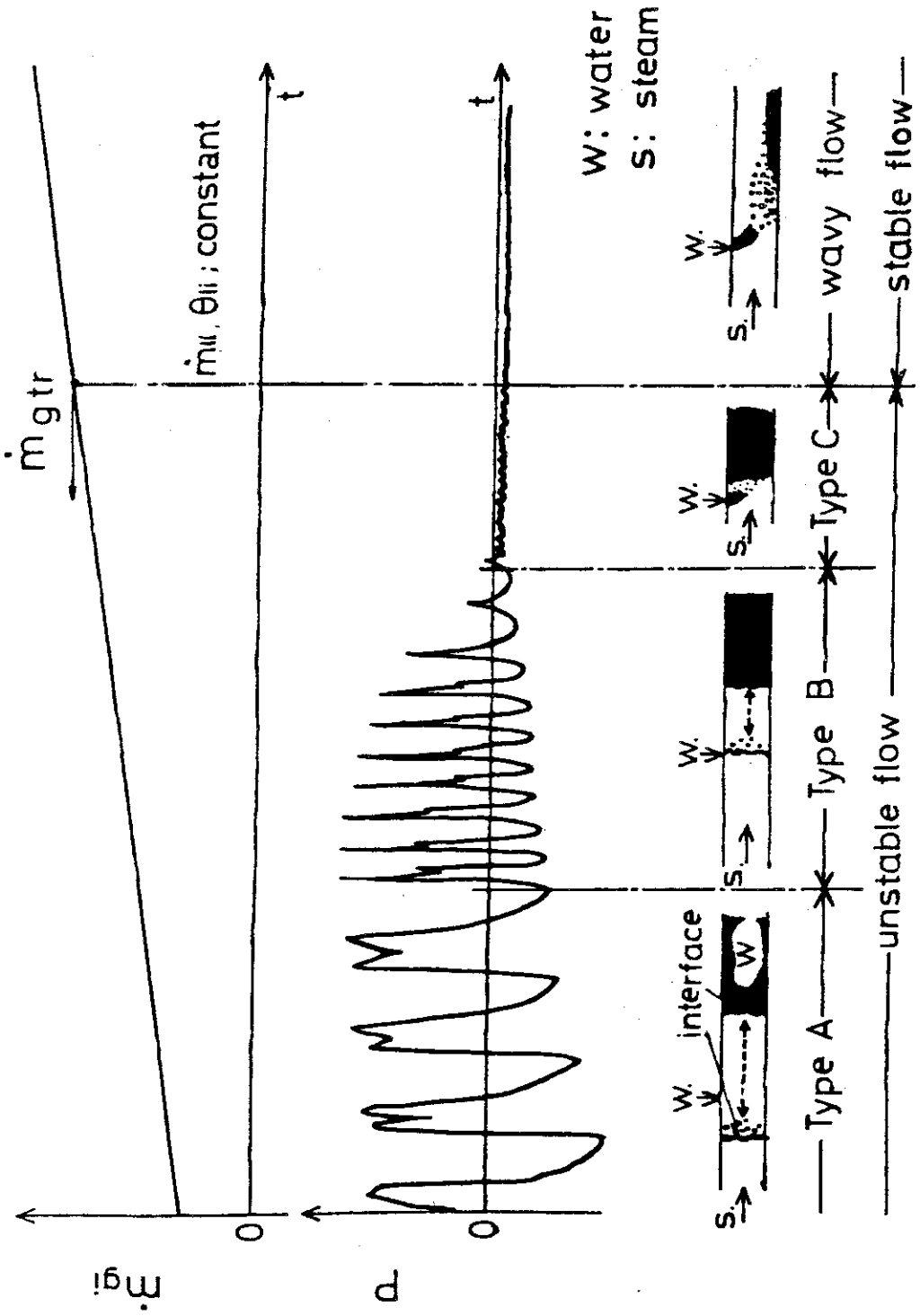

Figure 4 Pressure Oscillation and Flow Regime Transition from Reference 19

JAERI-M 9028 Errata

Page	Line	Printed	To be corrected
1	↑ 6	regime may used	regime map used
3	↑ 6	steam table.[22)]	steam table。
4	↑ 1	$-(\frac{\partial v}{\partial p})_T + v\kappa$	$-(\frac{\partial v}{\partial p})_T = v\kappa$
6	↓ 5	$g_p = (\frac{\partial g}{\partial x})_x$	$g_p = (\frac{\partial g}{\partial P})_x$
7	↓ 2	$\frac{dP(i)}{dt}$.	$\frac{dP(i)}{dt}$.
7	↓ 3	when subcooled	When subcooled
10	↓ 3	(Pvκ-Tvκ)	(Pvκ-Tvβ)
10	↑ 1	$P_{gs})\cdot(\frac{\partial T_g}{\partial P_{gs}})_{u_g}$	$P_{gs})(\frac{\partial T_g}{\partial P_{gs}})_{u_g}$
11	↓ 1	$P_{gs})\cdot(\frac{\partial v_g}{\partial P_{gs}})_{u_g}$	$P_{gs})(\frac{\partial v_g}{\partial P_{gs}})_{u_g}$
11	↑ 3	where $T_{\ell s}$,	Where $T_{\ell s}$,
12	↓19	cordinate of	coordinate of
13	↓ 3	transfer for	transfer[12)] for
15	↓ 8	may used.	may be used.
16	↓ 7	W_g $0.84M_{c,max}$	$W_g > 0.84M_{c,max}$
17	↑ 7	the friggering	the triggering
19	↓12	M_{COND}	$\dot{M}_{COND}$

日立高速印刷納